Wave Attenuation by Cultivated Seaweeds: a Linearized Analytical Solution

Yanlin Shao[a], **Morgane Weiss**[b], **Zhilong Wei**[a,*]
a. Department of Civil and Mechanical Engineering, Technical University of Denmark, 2800, Lyngby, Denmark
b. Swiss Federal Institute of Technology in Lausanne, 1015 Lausanne, Swiss
*Corresponding author. Email: zhilwei@dtu.dk

1 Introduction

An analytical framework is presented to describe the attenuation of regular and irregular waves propagating over floating seaweed farms. Kelp blades suspending on the longlines are modeled, as a first approximation, as rigid bars rotating around their upper ends. Assuming small-amplitude blade motions under low to moderate sea conditions, the frequency transfer function of the rotations can be obtained, with quadratic drag loads linearized. Subsequently, the hydrodynamic problem with regular waves propagating over suspended seaweed canopies is formulated using the continuity equation and linearized momentum equations with additional source terms within the vegetation region. Analytical solutions are obtained for the regular waves with their heights decaying exponentially as they propagate over the canopy. These analytical solutions are utilized as the basis to predict the wave attenuation of irregular waves while stochastic linearization of the quadratic drag loads is employed. The wave power spectral density is also seen to decay exponentially over the canopy. The present solutions can also be extended to include the elastic deformation of the vegetation blades.

2 Theory

We consider a 2D fluid domain in the xz-plane, with a submerged vegetation canopy which divides the whole fluid domain into three horizontal layers, as sketched in Fig. 1. The flow velocity and dynamic pressure in the jth fluid layer are defined as $\boldsymbol{u}_j = [u_j, w_j]$ and p_j, respectively. The heights of the layers are defined as d_j, $j = 1, 2, 3$. Right-going waves along the x-direction are considered. Their wave lengths and amplitudes change gradually as they propagate over the canopy due to the inertia and drag loads on the kelp blades, modelled as rigid rotating bars as a first approximation.

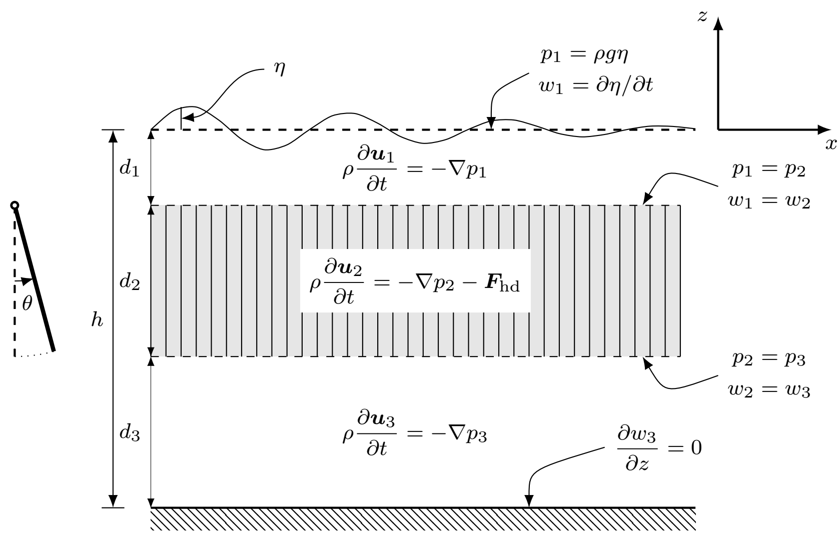

Figure 1: Governing equations in each layer, boundary conditions on the interfaces, and the sketch of a rigid bar pinned at the top. In Layer $j = 1, 2, 3$, p_j is the dynamic pressure, $\boldsymbol{u}_j = [u, w]$ is the velocity vector, d_j is the layer height. Inside the vegetation region (shaded area), an extra source term due to the presence of vegetation, $\boldsymbol{F}_{\mathrm{hd}}$, is added to the linearized momentum equation. $h = d_1 + d_2 + d_3$ is the water depth, η is the free-surface elevation, and ρ is water density. θ is the angle between the rigid bar and the downward vertical direction. t denotes time.

2.1 Small-Amplitude Rotational Motion of a Rigid Bar in Regular Waves

As illustrated in Fig. 1, a rigid bar pinned at the top is fully submerged in water. There is one single degree of freedom θ, the angle between the bar and the downward vertical direction. Morison's equation is used to calculate the hydrodynamic loads on it. The structure density ρ_s is assumed to be larger than the water density ρ, i.e., $\rho_s > \rho$. As a result, the equivalent gravity in water is always negative and acts as a restoring force. Assuming small-amplitude motion, i.e. $\theta \ll 1$, the moment balance between the hydrodynamic loads and equivalent gravity on the rigid bar yields

$$\left(I + \frac{1}{3}m_a l^3\right)\ddot{\theta} + \frac{1}{3}B^v l^3\dot{\theta} + \frac{1}{2}M' g l\theta = -B^v\int_{z_0}^{z_0-l} u_2(z_0 - z)\mathrm{d}z - m_a\int_{z_0}^{z_0-l}\frac{\partial u_2}{\partial t}(z_0 - z)\mathrm{d}z, \quad (1)$$

where l is the length of the bar, I is the moment of inertia of the pendulum about the pivot point, $z_0 = -d_1$ is the vertical position where the bar is pinned, $M' = (\rho_s - \rho)lS$ is the equivalent gravity in water and S is the cross-section area, $m_a = \pi\rho C_M b^2/4$ and b is the span width of the bar. B^v is the equivalent damping determined by

$$\frac{1}{2}\rho C_D b\int_{z_0}^{z_0-l}\int_0^T |u_2 - s\dot{\theta}|^3\mathrm{d}z\mathrm{d}t = B^v\int_{z_0}^{z_0-l}\int_0^T (u_2 - s\dot{\theta})^2\mathrm{d}z\mathrm{d}t, \quad (2)$$

where $s = -z - z_0$ is the distance to the pinned top. C_M and C_D are the inertia and drag coefficients. The Froude-Krylov force has been neglected here since the seaweed blade is quite thin. The wave-radiation damping is ignored as it is negligibly smaller than the viscous damping.

If the local ambient horizontal velocity u_2 can be approximated by a linear wave theory, a steady-state solution can be obtained for Eq. (1). Let Θ be the complex response amplitude of θ and H_Θ be the corresponding transfer function.

2.2 Analytical Solution to Regular Waves over Flexible Canopies

The general procedure of the analytical solution in each layer is briefly introduced here. We assume that the wave height decays *exponentially* as a function of horizontal distance x over the canopy. The dynamic pressure takes the form of

$$p_j = \Re\left\{P_j(d_j, \omega, H, \ldots; z)e^{\mathrm{i}(\omega t - kx)}\right\}, \quad (3)$$

where P_j is the complex amplitude function of z but not x or t, $k = k_r + \mathrm{i}k_i$ is the complex wave number, H is the wave height, and ω is the wave frequency. In addition, i is the imaginary unit. The velocity components u_j and w_j have similar expressions, and their corresponding complex amplitude functions U_j and W_j can be expressed in term of P_j from the linearized momentum equations. A linear ordinary differential equation (ODE) of P_j is given from the continuity equation in each layer. The ODEs of P_j are solved with the boundary conditions, as summarized in Fig. 1. Linear free-surface conditions and zero-Neumann condition are satisfied on the calm-water surface and a horizontal seafloor. On the interfaces between different fluid layers, the vertical velocity and the pressure are continuous across the layers.

Here we give the derivation details in Layer 2 (or the vegetation layer). Since small-amplitude motions are assumed, we only consider the horizontal hydrodynamic load. In addition, the interfaces between the canopy region and the water columns are also linearized onto $z = -d_1$ and $z = -(d_1 + d_2)$. In Layer 2, where $-d_1 - d_2 < z < -d_1$, the continuity equation is given by

$$\frac{\partial u_2}{\partial x} + \frac{\partial w_2}{\partial z} = 0. \quad (4)$$

The linearized momentum equations without convection and diffusion terms are considered, but with additional source terms to account for the presence of the canopy:

$$\frac{\partial u_2}{\partial t} = -\frac{1}{\rho}\frac{\partial p_2}{\partial x} - \frac{F_x}{\rho}, \quad \frac{\partial w_2}{\partial t} = -\frac{1}{\rho}\frac{\partial p_2}{\partial z}. \quad (5)$$

Here, F_x is the horizontal force per unit volume on the canopy given by Morison's equation

$$F_x = \rho C_M \frac{\pi b^2}{4} N \left(\frac{\partial u_2}{\partial t} - s\ddot{\theta} \right) + \frac{1}{2} \rho C_D b N |u_2 - s\dot{\theta}| (u_2 - s\dot{\theta}), \tag{6}$$

where b is the characteristic width of the blade, N is the number of the canopy components per unit horizontal area, i.e. canopy density. Plugging Eq. (6) into the horizontal momentum equation in Eq. (5), and linearizing the drag term will lead to

$$(1 + A) \frac{\partial u_2}{\partial t} = -\frac{1}{\rho} \frac{\partial p_2}{\partial x} + A s\ddot{\theta} - D(u_2 - s\dot{\theta}), \tag{7}$$

with

$$D = \frac{\int_{-d_1-d_2}^{-d_1} \overline{\frac{1}{2} C_D b N |u_2 - s\dot{\theta}|^3} \mathrm{d}z}{\int_{-d_1-d_2}^{-d_1} \overline{(u_2 - s\dot{\theta})^2} \mathrm{d}z}, \quad A = C_M \frac{\pi b^2}{4} N, \tag{8}$$

where the overbar means time averaging. D can be obtained through an iterative method.

Combining Eqs. (3), (5) and (7), one has

$$U_2 = \frac{1}{\rho} \frac{\mathrm{i}k}{\mathrm{i}\omega(A+1) + D} P_2 + \omega \frac{\omega A - \mathrm{i}D}{\mathrm{i}\omega(A+1) + D} \Theta(d_1 + z), \quad W_2 = \frac{\mathrm{i}}{\rho\omega} \frac{\mathrm{d}P_2}{\mathrm{d}z}. \tag{9}$$

Inserting the equations above into the continuity equation Eq. (4) gives

$$\frac{\mathrm{d}^2 P_2}{\mathrm{d}z^2} - \kappa^2 P_2 = \rho k \omega^2 \frac{A\omega - iD}{i\omega(A+1) + D} \Theta(z + d_1), \quad \left(\frac{\kappa}{k}\right)^2 = \frac{\mathrm{i}}{\mathrm{i}(A+1) + D/\omega}. \tag{10}$$

Similarly, the linear ordinary differential equations for P_1 and P_3 can be found. With the boundary conditions on the free surface, two interfaces, and the bottom, P_j can be solved. In addition, the dispersion relation reads

$$\omega^2 \left(1 + \frac{k}{\kappa^2} \frac{A\omega - iD}{i\omega(A+1) + D} H_\Theta \left(H_1 - T H_2 \right) \right) = gkT, \tag{11}$$

where

$$\begin{aligned} H_1 = {} & k d_2 \sinh(k d_1) \cosh(\kappa d_2) + \kappa d_2 \cosh(k d_1) \sinh(\kappa d_2) + \cosh k d_1 \\ & - \frac{k}{\kappa} \sinh(k d_1) \sinh(\kappa d_2) - \cosh(k d_1) \cosh(\kappa d_2), \end{aligned} \tag{12}$$

$$\begin{aligned} H_2 = {} & k d_2 \cosh(k d_1) \cosh(\kappa d_2) + \kappa d_2 \sinh(k d_1) \sinh(\kappa d_2) + \sinh k d_1 \\ & - \frac{k}{\kappa} \cosh(k d_1) \sinh(\kappa d_2) - \sinh(k d_1) \cosh(\kappa d_2), \end{aligned} \tag{13}$$

$$T = \frac{\tanh(k d_1) + \tanh(k d_3) + \frac{\kappa}{k} \tanh(\kappa d_2) + \frac{k}{\kappa} \tanh(k d_1) \tanh(\kappa d_2) \tanh(k d_3)}{1 + \tanh(k d_1) \tanh(k d_3) + \frac{\kappa}{k} \tanh(k d_1) \tanh(\kappa d_2) + \frac{k}{\kappa} \tanh(\kappa d_2) \tanh(k d_3)}. \tag{14}$$

If $H_\Theta = 0$, Eq. (11) reduces to the one for waves over rigid canopies, given in [2].

2.3 Analytical Solution to Irregular Waves over Flexible Canopies

In irregular waves, following the method of stochastic linearization, the damping is linearized as

$$D = \frac{1}{2} C_D b N \sqrt{\frac{8}{\pi}} \frac{\int_{-d_1-d_2}^{-d_1} \sigma_{u_{2,r}}^3 \mathrm{d}z}{\int_{-d_1-d_2}^{-d_1} \sigma_{u_{2,r}}^2 \mathrm{d}z}, \tag{15}$$

where $\sigma_{u_{2,r}}$ is the standard deviation of the relative velocity in Layer 2. Meanwhile, B_v in Eq. (2) should be linearized in this way as well. Since we assume that the wave height decays *exponentially* as a function of horizontal distance x over the canopy, i.e.,

$$\frac{H(x + \mathrm{d}x)}{H(x)} = \exp(k_i(\omega, x) \mathrm{d}x), \tag{16}$$

which is also the transfer function of wave height at $x + \mathrm{d}x$, the wave spectrum along the canopy will be

$$S(\omega, x + \mathrm{d}x) = S(\omega, x) \exp(2k_i(\omega, x)\mathrm{d}x). \tag{17}$$

This equation is then used together with a simple numerical procedure to obtain the wave spectrum at any location. If k_i is assumed as constant over x, which is not mandatory in the present derivation, Eq. (17) reduces to the same formula given by [2]

$$S(w, x) = S(w, x = 0) \exp(2k_i(\omega, x = 0)x), \tag{18}$$

where k_i is only evaluated at $x = 0$. Note also that our derivation also includes inertia forces on the vegetation, which has been ignored in [2].

3 Results

The analytical model is compared with experiments by [1] on irregular wave attenuation over a submerged canopy. The wave conditions are based on a single peaked JONSWAP spectrum with a peak enhancement factor $\gamma = 3.5$ and peak wave period $T_p = 1.15\,\mathrm{s}$. The incident significant wave height at the beginning of the canopy is $H_{s0} = 3.7\,\mathrm{cm}$ and the water depth is $0.685\,\mathrm{m}$. In our investigation, we focus solely on the thickest artificial vegetation blades and treat them as rigid bars. The vegetation blades were $0.26\,\mathrm{m}$ long and $4\,\mathrm{mm}$ wide with a density of $2264\,\mathrm{blades/m^{-2}}$.

The wave decay coefficient k_i predicted by our analytical model aligned with the experimental data, exhibiting a slight underestimation. See the left plot in Fig. 2. The discrepancy could potentially arise from skin friction along the glass sidewalls and the flume floor. The effect of the inertia forces is also investigated by using added mass coefficients $C_M = 0$ and 1. A constant drag coefficient $C_D = 1.95$ is assumed. $C_M = 1$ leads to a slightly smaller damping coefficient k_i. The wave spectrum at $x = 50\,\mathrm{m}$, approximately 24 peak-wave lengths into the canopy, is compared with that of the unattenuated waves at $x = 0\,\mathrm{m}$ in the right plot of Fig. 2. Significant wave attenuation is observed for the considered wave condition and canopy. The accumulated effect of the inertia forces can also be seen, which tends to reduce the wave attenuation. More results will be shown in the workshop.

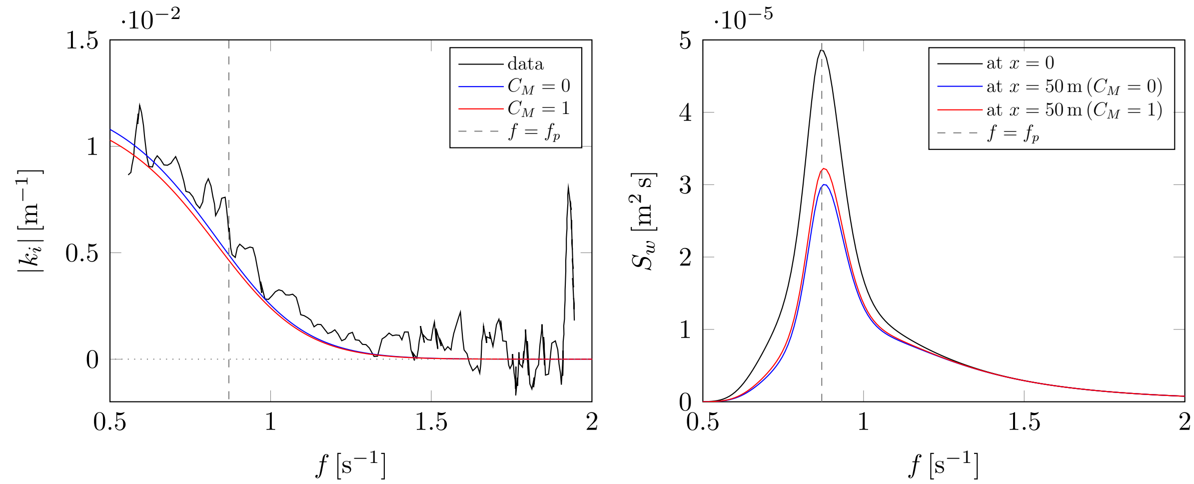

Figure 2: (left) Comparison of wave decay coefficient k_i at $x = 0$ where the canopy starts. (right) Initial wave spectrum and decayed wave spectra at $x = 50\,\mathrm{m}$. Note that when $C_M = 0$, the present model will be reduced to the one given in [2]. $C_D = 1.95$ for all frequencies.

References

[1] Jacobsen, N., McFall, B. and van der A, D. [2019], 'A frequency distributed dissipation model for canopies', *Coastal Engineering* **150**, 135–146.

[2] Zhu, L. [2020], Wave Attenuation Capacity of Suspended Aquaculture Structures with Sugar Kelp and Mussels, PhD thesis, The University of Maine.